Evaluation of Carotid Artery Segmentation with Centerline Detection and Active Contours without Edges Algorithm

Tomasz Hachaj, Marek R. Ogiela

Evaluation of Carotid Artery Segmentation with Centerline Detection and Active Contours Without Edges Algorithm

Tomasz Hachaj[1], Marek R. Ogiela[2]

[1] Pedagogical University of Krakow, Institute of Computer Science and Computer Methods, 2 Podchorazych Ave, 30-084 Krakow, Poland, tomekhachaj@o2.pl
[2] AGH University of Science and Technology 30 Mickiewicza Ave, 30-059 Krakow, Poland, mogiela@agh.edu.pl

Abstract. The main contribution of this article is a new method of segmentation of carotid artery based on original authors inner path finding algorithm and active contours without edges segmentation method for vessels wall detection. Instead of defining new force to being minimized or intensity metric we decide to find optimal weight of image – dependent forces. This allows our method to be easily reproduced and applied in other software solutions. We judge the quality of segmentation by dice coefficient between manual segmentation done by a specialist and automatic segmentation performed by our algorithm. We did not find any other publication in which such approach for carotid artery bifurcation region segmentation has been proposed or investigated. The proposed algorithm has shown to be reliable method for that task. The dice coefficient at the level of 0.949±0.050 situates our algorithm among best state of the art methods for those solutions. That type of segmentation is the main step performed before sophisticated semantic analysis of complex image patterns utilized by cognitive image and scene understanding methods. The complete diagnostic record (Electronic Health Record – EHR) obtained that way consists private biometric data and its safety is essential for personal and homeland security.

Keywords: Active contours without edges, lumen segmentation, carotid bifurcation, computed tomography angiography, brain perfusion maps, computer - aided diagnosis.

1 Introduction

Extracting vessels from computed tomography angiography (CTA) is a key requirement for the display and analysis that type of modality [1]. CTA is a popular medical imaging method that is often used beside standard computed tomography (CT) in acute stroke imaging. Imaging of the carotid arteries is important for the evaluation of patients with ischemic stroke or Transient Ischemic Attack (TIA). There are many automatic methods to perform the task of segmentation that have been yet proposed in literature. That methods can be divided into two groups: model – based and intensity – based. The first group analysis the geometric specificity of vessels, in particular the

notions of orientation and tubular shape. The common approach is utilizing some tube detection filters based on analysis of volume Hessian matrix eigenvalues [2]. Those methods are capable to detect any local tubular structure but are sensitive to noises and scanning artifacts. Algorithms among the second group are dedicated mainly for detailed extraction of continues tubular structures. Many of those algorithms are two – step procedures: at first algorithm finds the path within examined vessel, than detects its boundary. In [3] authors finds minimal cost paths between the Common Carotid Artery (CCA) and both the External Carotid Artery (ECA) and the Internal Carotid Artery (ICA). Then the cylindrical tube around each path is created with a radius of 0.5mm that is later used for the level set evolution algorithm with proper function of the image intensity. Method in [4] is based on a variant of the minimal path method that models the vessel as a centerline and boundary. This is done by adding one dimension for the local radius around the centerline. The crucial step of method is the definition of the anisotropic metric giving higher speed on the center of the vessels and also when the minimal path tangent is coherent with the vessels direction. Segmentation is refined using a region-based level sets.

The main contribution of this article is a new method of segmentation of carotid artery based on original authors inner path finding algorithm and active contours without edges segmentation method for vessels wall detection. Instead of defining new force to being minimized or intensity metric we decide to find optimal weight of image – dependent forces. This allows our method to be easily reproduced and applied in other software solutions. We judge the quality of segmentation by dice coefficient between manual segmentation done by a specialist and automatic segmentation performed by our algorithm. We did not find any other publication in which such approach for carotid artery bifurcation region segmentation has been proposed or investigated.

That type of segmentation is the main step performed before sophisticated semantic analysis of complex image patterns utilized by cognitive image and scene understanding methods. The complete diagnostic record (Electronic Health Record – EHR) obtained that way consists private biometric data and its safety is essential for personal and homeland security.

The results presented in this article are extension of our previous work. Our latest researches were concentrated on automatic analysis of dynamic perfusion computed tomography maps (CTP) in the event of brain stroke [5]. We decided to widen the area of our interest on CTA because the examination of carotid arteries is an important step during assessing the risk of brain stroke [6].

2 Methods

The proposed lumen segmentation method is consisted of two sub-algorithms. After preprocessing step the first algorithm detects the possible path between the start and the end point (it is similar to typical region growing algorithm). In the second step it performs the thinning of previously obtained path. The generated path between the start and point becomes 1 voxel width keeping the same length as path from first step. The second algorithm is an active contours without edges segmentation method. The role of this procedure is to segment the whole lumen of considered vessel. The active

contours is computed in axial slices and the starting counter is the sphere with radius of 5 voxels. The center point of each sphere is a voxel taken from path from Algorithm I. The algorithm requires manual indication of two initial points inside both sides of vessel to be segmented. In order to detect bifurcated structures (like CCA – ICA – ECA) three points have to be chosen and the path detection algorithm have to be run two times, ones for CCA – ICA part than for CCA – ECA. After computing both paths the further analysis is performed on all voxels from both obtained paths.

List of symbols used in algorithm description:

Freezed points:= $\bullet$ *– already visited points.*

Narrow band$_i$*:=* $\bullet$ *– points, that are visited in i-th step.*

Start point – starting point of the path. $\bullet$

End point – end point of the path.

Delta value:=0 - maximal accepted difference between neighbor points.

S(x_j) *- Surrandings of point* x_j *with radius 1 (26 voxels).*

V(x_j) *- Value of vexel density in point* x_j.

Path length - the length of the path (in voxels).

Delta value - maximal accepted difference between two voxel densities. If the difference is greater than Delta value, the considered voxel is not included into the path.

In the preprocessing step of first algorithm the volumetric image is convoluted with Gaussian kernel in order to remove noises and scanning artifacts. The image is then thresholded in order to remove voxels that density do not belongs to range:

[min(V(Start point), V(End point)) – 40, max(V(Start point), V(End point)) + 200]

That step eliminates the uncontrolled propagation of path detection algorithm in regions where tissues has too low or too high density to be part of examined vessel.

Algorithm I, step I – detection of path between *Start point* and *End point*.

```
Delta value:=-1
While (End point∉Freezed points)
  Delta value:=Delta value+1
i:=0
Narrow band:= •
Narrow band0:={Start point}
Freezed point:={(Start point, I)}
While ( #Narrow bandi>0 ∧ End point ∉Freezed points)
i:=i+1
∀xj∈Narrow bandi
∀yk∈S(xj)
  if(|V(xj)- V(yk)|<Delta value)
    Narrow bandi:= Narrow bandi∪ yk
    Freezed point:= Freezed pointi∪ (yk, i)
Path length:=i
```

End algorithm I, step I

Because the algorithm stops immediately after detecting the end point it will not generate paths that are too long and it is unnecessary to add any penalization term of path length to the edges weighting function.

Algorithm I, step II – thinning of path obtained in step I. The path generated in second step has the same length as previous path but is only one voxel width.

```
Path:= • – path from End point to Start point
Path:=Path∪End point
k:=Path length -1
i:=0
x_i:=End point
While(Start point ∉ Path)
  X_{i+1}:=(y_j: |V(y_j)-V(x_i) |=min|V(y_1)-V(x_i) |, (y_1,k) ∈Freezed
points, y_1∈S(x_i))
  Path:= Path∪x_{i+1}
  i:=i+1
  k:=k-1
End Algorithm I, step II
```

The second algorithm is based on active contours without edges segmentation procedure [7]. The method requires rescaling the CT volume ISO values (densities) so that it does not consist any negative values of voxels. Beside of that the active contours algorithm does not require any preprocessing and is performed on “raw” CT volume data

The basic idea in active contours models or snakes is to evolve a curve, subject to constraints from a given image in order to detect objects in that image [7]. Let Σ be a bounded open subset of R^2. The algorithm is driven by optimization procedure of energy term:

$$F_1(C,c_1)+F_2(C,c_2)=\int_{inside(C)}\left(I(x,y)-c_1\right)^2+\int_{outside(C)}\left(I(x,y)-c_2\right)^2 \quad (1)$$

Where:
C is the curve that represents the boundary of segmented region in Σ.
I(x,y) is pixel intensity value of image to be segmented with coordinates x, y.
c_1 is average value of pixels intensity inside region with boundary C.
c_2 is average value of pixels intensity outside region with boundary C.

The equation (1) may also consist regularization terms [7] and becomes:

$$F(c_1,c_2,C) = \mu \cdot Length(C) + \nu \cdot Area(inside(C)) + \lambda_1 \int_{inside(C)} |I(x,y) - c_1|^2 dxdy + \lambda_2 \int_{outside(C)} |I(x,y) - c_2|^2 dxdy \quad (2)$$

The first term depends on length of the curve, the second on area inside it. Parameters :, <, 8_1 and 8_2 ($\mu, \nu \geq 0$, $\lambda_1, \lambda_2 > 0$) are constants.

In [8] the authors proposed an effective implicit representation for evolving curves and surfaces, which has found many applications, because it allows for automatic change of topology such as merging and breaking, and the calculations are made on a fixed rectangular grid. A given curve C is represented by zero level set of a scalar Lipschitz continuous function $\phi : \Omega \to R$ such that:

$$\begin{cases} C = \partial\omega = \{(x,y) \in \Omega : \phi(x,y) = 0\} \\ inside(C) = \omega = \{(x,y) \in \Omega : \phi(x,y) > 0\} \\ outside(C) = \omega = \{(x,y) \in \Omega : \phi(x,y) < 0\} \end{cases} \quad (3)$$

The energy from (2) might be rewritten as:

$$F(c_1,c_2,\phi) = \mu \int_\Omega \delta(\phi(x,y)) |\nabla \phi(x,y)| dxdy + \nu \int_\Omega H(\phi(x,y)) dxdy + \lambda_1 \int_\Omega |I(x,y) - c_1|^2 H(\phi(x,y)) dxdy + \lambda_2 \int_\Omega |I(x,y) - c_2|^2 (1 - H(\phi(x,y))) dxdy \quad (4)$$

Where:

$$H(z) = \begin{cases} 1 & if \quad z \geq 0 \\ 0 & if \quad z < 0 \end{cases} \quad (5)$$

H is the Heaviside function

$$\delta_0(z) = \frac{d}{dz} H(z) \quad (6)$$

Dirac measure.

In numerical solution the non-zero value of $*_0$ is defined in range $(z-\varepsilon, z+\varepsilon)$, where ε is a small $\varepsilon > 0$ value.

In the rest of this article we assume that $\nu = 0$ and we do not consider area regularization term into calculations.

In order to minimize $F(c_1, c_2, \phi)$ with respect to N we have to solve Euler-Lagrange equation for N [9].

$$\frac{\partial \phi}{\partial t} = \delta(\phi)\left(\mu \cdot div\left(\frac{\nabla \phi}{|\nabla \phi|} \right) - \lambda_1 (I - c_1)^2 + \lambda_2 (I - c_2)^2 \right) = 0 \text{ in } t \geq 0 \text{ and in } \Sigma$$

$$\phi(0, x, y) = \phi_0(x, y) \text{ in } \Sigma \tag{7}$$

$$\frac{\delta(\phi)}{|\nabla \phi|} \frac{\delta \phi}{\delta \bar{n}} = 0 \text{ in } \partial\Omega$$

Where:

$\bar{n}$ is the exterior normal of the boundary $\partial\Omega$

$\frac{\delta \phi}{\delta \bar{n}}$ is the normal derivative of N at the boundary.

The parameters < (curve smoothing term), 8_1 and 8_2 affects results of optimization procedure. In our case we wanted to verify the hypothesis that term 8_1 should have the higher value than 8_2 to perform proper lumen segmentation. That is because we wanted to restrain the excessive grown of segmented area especially when the borders between area of interest and another tissue with similar density is very narrow. In our experiment the smoothing term is set to $\mu = 0.55$ that we assumed proper for considered segmentation task.

3 Results

The proposed algorithm was tested on a set of four CTA volumes of carotid artery with size 512x512x415, 512x512x425, 512x512x432 and 512x512x433 voxels scanned by SOMATOM Sensation 10 CT scanner. The distance between axial slices was 0.7 mm. The segmentation was performed on left and right carotid artery separately. Because of that the experimental set was consisted of eight tubular structures.

The volume to be segmented was determined similarly as in comparison protocol in [10]. It is defined around the bifurcation slice, which was marked as the first (caudal to cranial) slice where the lumen of the CCA appears as two separate lumens:

the lumen of the ICA and the lumen of the ECA (external carotid artery). The segmentation contain the CCA, starting at least 20 mm caudal of bifurcation slice, the ICA, up to at least 40 mm cranial of bifurcation slice, and the ECA, up to between 10 and 20 mm cranial of the bifurcation slice. The segmentation was performed at first on CCA – ICA section, than on CCA – ECA, the final segmentation result is the common part of those two. The 8_1 that we took into account was: 1, 2, 4, 6, 8 and 10. In figure 1 the carotid arteries segmentation results of all considered CTA volumes are presented ($\lambda_1 = 10$).

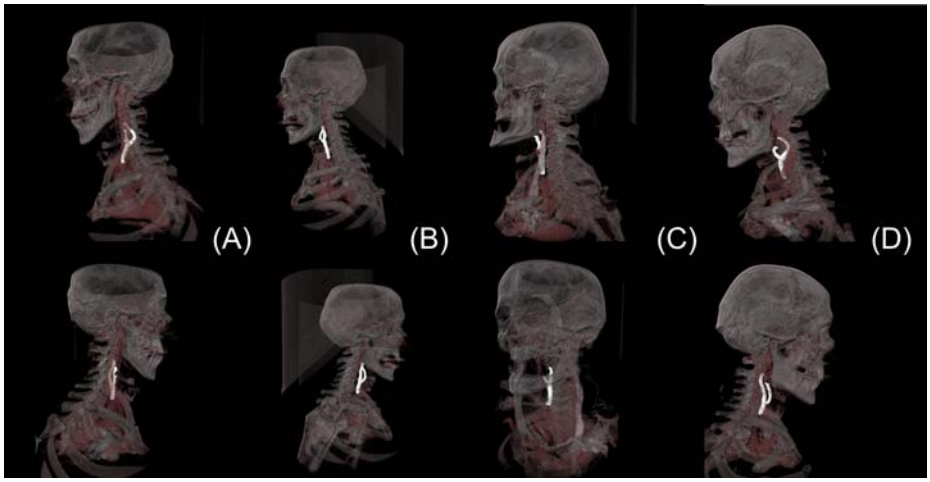

Fig. 1. The carotid arteries segmentation results of all considered CT volumes ($\lambda_1 = 10$). Each column consists different CTA volume. Top row visualize left carotid artery, the bottom the right one.

The TP, FP, TN and FN coefficients values as the function of 8_1 parameter for CTA from figure 1 (B), bottom row (right artery) are shown in table 1. The visualized results of the same artery are presented in figure 2 and figure 3.

Table 1. The TP, FP, TN and FN coefficients values as the function of 8_1 parameter for CTA from figure 1 B, bottom row (right artery).

81	TP	FP	TN	FN
1	12596	5380	116111768	48
2	12496	3538	116113610	148
4	12542	2042	116115106	102
6	12516	1223	116115925	128
8	12446	617	116116531	198
10	12427	238	116116910	217

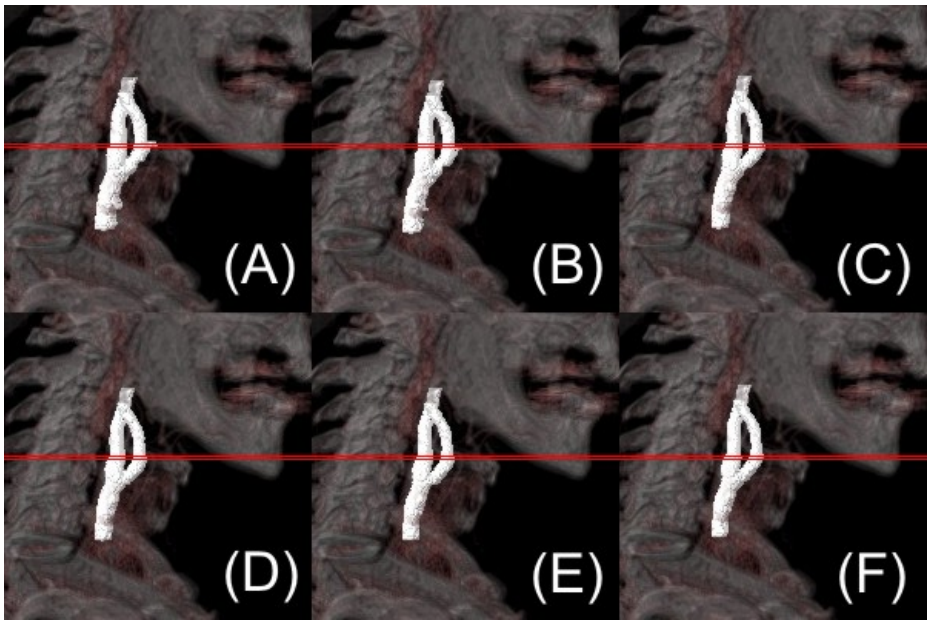

Fig. 2. Detailed view of segmentation results for CTA from figure 1 B, bottom row (right artery). Red line marks the axial slice that is presented later in figure 3.

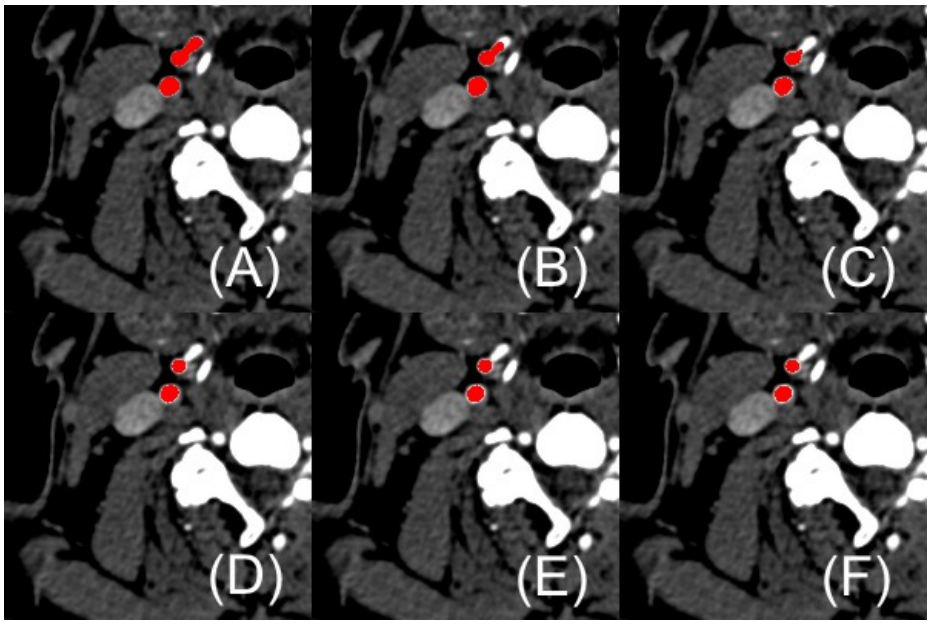

Fig. 3. Detailed view of segmentation results for CTA from figure 1 B, bottom row (right artery). Red regions are the segmented ICA and ECA tissues.

The volume lumen segmentations is evaluated using the dice similarity measure:

$$D_{si} = \frac{2 \cdot \left| pv_r \cap pv_p \right|}{\left| pv_r \right| + \left| pv_p \right|} \tag{8}$$

Where pv_r and pv_p are the reference and an algorithmically determined arteries tissues. Table 2 presents values of dice coefficient between manual segmentation performed by specialist and automatic segmentation performed by our algorithm. The last column consists average value of coefficient for all considered CTA volumes for given 8_1 value (± standard deviation).

Table 2. Values of dice coefficient between manual segmentation performed by specialist and automatic segmentation performed by our algorithm. The last column consists average value of coefficient for all considered CTA volumes for given 8_1 value (± standard deviation).

81\case	1	2	3	4	5	6	7	8	AVG
1	0.648	0.535	0.835	0.823	0.764	0.785	0.806	0.745	0.743±0.096
2	0.765	0.649	0.879	0.872	0.795	0.825	0.863	0.829	0.810±0.071
4	0.879	0.823	0.924	0.921	0.822	0.886	0.913	0.903	0.884±0.039
6	0.927	0.899	0.951	0.949	0.835	0.876	0.947	0.929	0.914±0.040
8	0.953	0.945	0.959	0.968	0.829	0.907	0.969	0.953	0.935±0.044
10	0.977	0.970	0.956	0.982	0.827	0.923	0.986	0.973	0.949±0.050

4 Discussion

The detail analysis of segmentation results (table 1) shows that increasing of 8_1 causes increasing of true negative (TN) and false negative (FN) classification of vessel tissues. From the other hand true positive (TP) and false positive (FP) coefficient decreases. That is because less voxels are captured into region surrounded by active contours during algorithms second step. That behavior is also clearly visible in figure 2 if we compare (A) and (F). The segmented region in (F) is thinner and it also does not consist additional false segmented tissue region. The same situation in the axial view is visualized in Figure 3 (A) and (F). The increasing of 8_1 parameter causes also as expected increase of dice coefficient as it is shown in table 2. From the value of 8_1 above 6 we observe the increasing of standard deviation between averaged results. That is because not always the higher value of 8_1 causes the improvement of segmen-

tation results (case 5 in table 2). That is because above some value the expansion of counters might be stopped by the force weighted by 8_2.

5 Conclusions

The proposed algorithm has shown to be reliable method for the task of carotid bifurcation region segmentation. The dice coefficient at the level of 0.949±0.050 situates our algorithm among best state of the art methods for those solutions. What is more our proposition can easily be implanted using popular image processing libraries that consists parameterizes active contours without edges algorithm. The proposed method has some drawbacks. The first is that the value of 8_1 that results in optimal from medical point of view solution may differ between examined CTA. The second one is long performance time of the segmentation procedure. What is more the first part of the algorithm – the path finding procedure may be difficult to parallelize on SIMD machines (like GPU processors) because that algorithm is highly sequential (not parallel). It is difficult to predict how the region growing procedure will evolve in each step.

Our method requires further investigation in order to find optimal value not only for 8_1 but also 8_2 and curvature – steering μ. The validation of the segmentation should be performed on bigger set of control data. If the result of evaluation will be on acceptable rate we will use this algorithm as the baseline for the further researches on automatic diagnosis of carotid structures. In order to accomplish this task we are planning to create appropriate semantic description of carotid artery similarly to those proposed in [11], [12]. After correct identification of possible lumen abnormality we will try to integrate the results with already developed by us CTP diagnosis framework. That approach will allow us to create more complex and complete diagnostic records (Electronic Health Record – EHR) that might be very helpful for radiologist in decision - making process. Nowadays EHR becomes a standard in hospital information systems and in the future might be accessed by wireless personal devices in the area of hospital using low-power personal area networks [13]. The proper information flow policy model will forbid a doctor from mixing the personal medical details of the patients [14]. What is more EHR consists private biometric data and its safety is essential for personal and homeland security.

Acknowledgments

We kindly acknowledge the support of this study by a Pedagogical University of Krakow Statutory Research Grant.

References

1. Josephson, S.A., Bryant, S.O., Mak, H.K., Johnston, S.C., Dillon, W.P., Smith, W.S.: Evaluation of carotid stenosis using CT angiography in the initial evaluation of stroke and TIA., Neurology. Aug 10;63(3):457-60, (2004)
2. Hachaj, T., Ogiela, M. R.: Segmentation and Visualization of Tubular Structures in Computed Tomography Angiography, Intelligent Information and Database Systems Lecture Notes in Computer Science, 2012, Volume 7198/2012, 495-503, DOI: 10.1007/978-3-642-28493-9_52, (2012)
3. Krissian, K., Arencibia Garcia, S.: A Minimal Cost Path and Level Set Evolution Approach for Carotid Bifurcation Segmentation, Proc. of MICCAI´09 Workshop: Carotid Lumen Segmentation and Stenosis Grading Challenge, (2009)
4. Mille, J., Benmansour, F., Cohen, L.: Carotid Lumen Segmentation Based on Tubular Anisotropy and Contours Without Edges, Proc. of MICCAI´09 Workshop: Carotid Lumen Segmentation and Stenosis Grading Challenge, (2009)
5. Hachaj T.: Pattern Classification Methods for Analysis and Visualization of Brain Perfusion CT Maps, Computational Intelligence Paradigms in Advanced Pattern Classification (Eds. Ogiela, Marek R.; Jain, Lakhmi C), Studies in Computational Intelligence, Vol. 386, p. 145-170, (2012)
6. Steinman, D.A., Poepping, T.L, Tambasco, M., Rankin, R.N., Holdsworth D.W.: Flow Patterns at the Stenosed Carotid Bifurcation: Effect of Concentric versus Eccentric Stenosis, Annals of Biomedical Engineering, Volume 28, Number 4, 415-423, DOI: 10.1114/1.279, (2000)
7. Chan, T. F., Vese, L. A.: Active contours without edges. IEEE Transactions on Image Processing, 10(2), 266-277, (2001)
8. Osher, S., Sethian, J.A.: Fronts propagating with curvature dependent speed: Algorithms based on Hamilton-Jacobi formulation. JCP, 79:12–49, (1988)
9. Chan, T. F., Vese, L. A.: A Multiphase level set framework for image segmentation using the Mumford and Shah model. International Journal of Computer Vision 50(3), 271–293, (2002)
10. Hameeteman, R., Zuluaga, M., Joskowicz, L., Freiman, M., Van Walsum, T.: Carotid lumen segmentation and stenosis grading challenge. Online, May 2009. 4.2, 5.1; http://cls2009.bigr.nl/download/evaluationframework2009.pdf
11. Trzupek, M., Ogiela, M.R., Tadeusiewicz, R.: Intelligent image content semantic description for cardiac 3D visualisations. Engineering Applications of Artificial Intelligence 24, 1410–1418, (2011)
12. Trzupek, M.: Semantic modelling of coronary vessel structures in computer aided detection of pathological changes. A M. Tjoa et al. (Eds.): ARES 2011, LNCS 6908, 2011, pp. 220–227, (2011)
13. Jara, A. J., Zamora, M. A., Skarmeta, A. F. G.: An Initial Approach to Support Mobility in Hospital Wireless Sensor Networks based on 6LoWPAN (HWSN6). Journal of Wireless Mobile Networks, Ubiquitous Computing, and Dependable Applications. Volume: 1. Number: 2/3. pp 107-122. ISSN: 2093-5374 (2010).
14. Viet Triem Tong, V., Clark, A. & Mé, L.: Specifying and enforcing a fine-grained information flow policy : model and experiments. Journal of Wireless Mobile Networks, Ubiquitous Computing, and Dependable Applications, 1(1), pp. 56-71 (2010)